ACS OMEGA

Open Access

http://pubs.acs.org/journal/acsodf

Article

Laboratory Evaluation of a Low-Damage Authigenic Mud Acid System for Bai-823 Well Block

Xiaolong Ni, Runxin Cao, Weifeng He, Jinming Zhao, and Chaozong Yan*

Cite This: *ACS Omega* 2023, 8, 46490−46498

Read Online

ACCESS | Metrics & More | Article Recommendations

ABSTRACT: Aiming at the problem of single and poor adaptability of Bai-823 plugging removal system, an authigenic mud acid system using methyl formate, ammonium chloride, and ammonium fluoride as raw materials is proposed, which can adapt to the temperature of 60−80 °C of the target reservoir and sandstone lithology. The acid-generating capacity of the authigenic acid system at different temperatures was evaluated. The results showed that the H^+ concentration remained at 3.35 mol/L after 180 min at 80 °C, which indicated that authigenic acid could generate acid continuously and thus be competent for acidizing and plugging removal of further wells. The corrosion rate of authigenic acid to N80 steel was further investigated. When 2 wt % SA1-3B corrosion inhibitor was used, the corrosion rate was only 0.15 g/(m^2·h). At the same time, the corrosion capacities of authigenic acid to rock core and scale samples were studied, which were 19.38 and 93.81%, respectively, indicating that the authigenic acid system realized pipeline and reservoir friendliness when it was able to effectively remove plugging. Finally, a core displacement experiment was carried out to simulate reservoir acidizing for plugging removal. The results showed that the core permeability increased from 1.00 to 1.63 after acidizing modification with authigenic acid. All of the above studies show that a kind of authigenic mud acid has been successfully prepared, and a new idea for the authigenic acid system has been proposed.

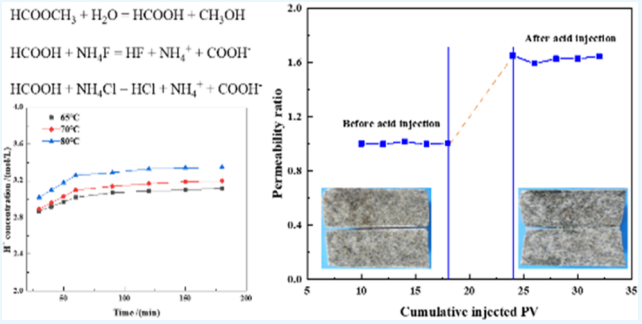

1. INTRODUCTION

In recent years, the world economy has developed rapidly, and the global demand for oil and gas has also increased year by year. Currently, in order to increase oil and gas production capacity, many countries and regions, including China, have had to shift their development goals toward low-permeability and tight reservoirs, as well as carry out refracturing transformation on developed areas.[1] Among them, low-permeability and tight reservoirs often have problems such as poor reservoir properties, small pore throats, and severe heterogeneity; when refracturing a reservoir that has already been modified, it is easy to encounter problems such as pore throat and crack blockage caused by incomplete gel breaking or mismatched physical properties of the reservoir during the previous modification.[2,3] In a word, conventional fracturing makes it difficult to achieve the expected reservoir reconstruction effect. At this time, the retarded acid must be used to unblock the target reservoir to improve the reconstruction effect.

The retarded acid is an important way for reservoir acidification and plugging removal.[4,5] Its main mechanism is to extend the fractures in the formation through acid dissolution,[6,7] dredge the seepage channel of rocks,[8,9] and dissolve the solid impurities in the formation[10,11] so as to restore or improve productivity. Over the years, many scholars have studied this technology. Nazari et al.[12] introduced a new retarded acid system, which is mainly composed of hydrochloric acid and chloroacetic acid sodium salt. The main advantage of this retarded acid is that it can be applied without gel through polymer or surfactant or emulsification in diesel oil. Abdrazakov et al.,[13] based on the former Caspian Depression in Kazakhstan, combined with the data and geological conditions of the construction site, studied the retarded acid through experimental research and software simulation, and developed a set of retarded acid systems that can adapt to a depth of up to 5000 m and a temperature of up to 145 °C. Ravichandran et al.[14] developed a highly slow-moving single-phase acid and applied it to several gas wells in the offshore gas field of East Malaysia, achieving significant improvement results.

Autogenic acid is a kind of retarded acid,[15,16] which can also be called potential acid. Generally, it is a special acid solution

Received: July 4, 2023
Revised: November 6, 2023
Accepted: November 14, 2023
Published: November 30, 2023

system with different types of acids formed by the reaction of several nonacidic or weak acidic substances under specific environmental conditions.[16−18] Compared with other types of retarded acid, it has the characteristics of lower acidity on the ground, which leads to lower corrosivity of authigenic acid when it enters the string, so it can protect the string more effectively. At the same time, since the acid generation reaction of autogenic acid is gradual, it means that the autogenic acid system will not have the problem of rapid acid deactivation, and it is more suitable for plugging removal and production increase in further well zones.[19,20] At present, according to the different types of acid generation, autogenic acid can be roughly divided into autogenic hydrofluoric acid, autogenic hydrochloric acid, autogenic organic acid, and composite autogenic acid systems.[19,,22]

Keshang Formation oil reservoir in the Bai-823 well area in Xinjiang is located about 10 km to the east of the Baijiantan District. It is characterized by poor physical properties of the reservoir, mainly fine pore throat, poor sorting, poor damage tolerance, argillaceous cementation of the rock, potential salt sensitivity, medium to strong water sensitivity, sodium bicarbonate water type of formation, and easy scaling. And the reservoir temperature is low, which is distributed in the range of 60−80 °C. In addition, the core data of the well shows that the main lithology of the Keshang Formation is gray sandy small conglomerate, gravelly coarse sandstone, gravelly sandstone, medium fine sandstone, and mudstone, of which the sandstone is mainly composed of quartz and feldspar. The main component of the filler matrix is kaolinite, the main component of the cement is calcite, and the cementation is mainly compression type. Now, the single well in the work area has some problems, such as special damage shape, great difficulty in plugging removal due to uneven profile, single plugging removal system and process in the early stage, and poor adaptability.

In view of the above problems, an authigenic mud acid system is proposed. The system uses methyl formate, ammonium chloride, and ammonium fluoride as raw materials, which can be perfectly applied to the low temperature and lithology of the target reservoir. Meanwhile, reservoirs with similar physical properties to the target block, especially those with lower temperatures, can also be inspired by this study. The acid generation ability, static dissolution ability, and plugging removal performance of core displacement simulation acidification are evaluated for this authigenic mud acid system.

2. MATERIALS AND METHODS

2.1. Materials. Hydrochloric acid and hydrofluoric acid are electronic upgrades, purchased from Chengdu Chron Chemicals Co.; sodium hydroxide is analytically pure and purchased from Chengdu Chron Chemicals Co.; methyl formate (95 wt %) is purchased from Shanghai Maclin Biochemical Technology Co.; ammonium fluoride as AR is purchased from Shanghai Maclin Biochemical Technology Co.; corrosion inhibitor SA1-3B industrial product (78 wt %) is supplied by oilfield.

2.2. Preparation of Acid for the Experiment. A certain amount of deionized water was weighed in a plastic beaker, and then methyl formate, ammonium chloride, and ammonium fluoride in the molar ratio of 1:1:0.3 were mixed, and the authigenic mud acid was started at a specific temperature, after the three agents were dissolved evenly in deionized water. The specific configuration process is shown in Figure 1. Another

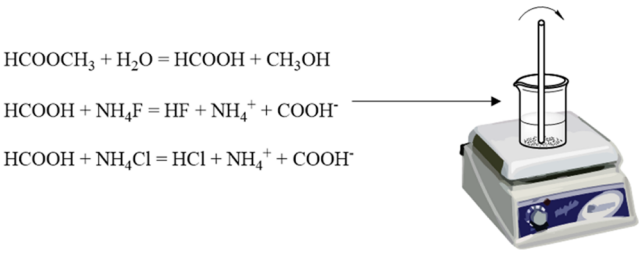

Figure 1. Configuration process of authigenic mud acid and authigenic acid mechanism.

volumetric flask was added with 10 wt % hydrochloric acid and 3 wt % hydrofluoric acid, and then deionized water was added to fix the volume to prepare the mud acid, which was used in the subsequent comparison experiments.

2.3. Experiment on the Evaluation of the Acid-Generating Capacity of Authigenic Acid. Acid generation capacity is the change in the concentration of H^+ ions in the authigenic acid system with increasing time. A standard solution of NaOH at 1.0 mol/L was used to titrate the authigenic acid mixture with the addition of phenolphthalein, and the change in H^+ concentration in the authigenic acid system with time was calculated by the consumption of lye. The formula for calculating H^+ is shown in eq 1.[23,24]

$$C_{acid} = \frac{C_{NaOH} \times V_t}{V_{acid}} \quad (1)$$

where C_{acid} is the H^+ concentration in the acid system, mol/L; C_{NaOH} is the OH^- concentration in the lye system, mol/L; V_t is the volume of lye for titration, mL; and V_{acid} is the acid volume, mL.

2.4. N80 Steel Static Corrosion Test.

(1) Put the prepolished smooth N80 steel in the model cleaner, clean it, air-dry it, and then put it into the dryer for about 20 min and weigh it.
(2) Prepare 300 mL of acid solution, add the acid solution to the bottle, tie the steel piece with a string, and suspend it in the bottle containing the acid solution. Put it into a 65 °C water bath for 4 h.
(3) Wash the reacted steel pieces in the model cleaner, soak in ethanol solution for 5 min, air-dry, put it into a dryer to dry, and then weigh their mass after cooling.
(4) The formula for calculating the average corrosion rate of steel is shown in eq 2.

$$V_1 = 10^{-4} \times \frac{W}{A \times t} \quad (2)$$

where V_1 is the average corrosion rate of steel, g/(m^2·h); W is the weight loss of steel, g; A is the exposed area of the steel, i.e., the area in contact with the acid, cm^2; and t is the corrosion time, h.

2.5. Experiment on the Dissolution Ability of Acid on Scale Samples.

(1) The Bai-823 scale sample was pounded and ground, passed through an 80 mesh sieve, dried at 100 °C for 24 h, placed in a dryer, and set aside.
(2) The filter paper was dried and cooled in a desiccator, and the mass of the filter paper m_1 was weighed.
(3) The scale sample powder with a mass of m_2 (about 2 g is recommended) was weighed and placed in a beaker.

https://doi.org/10.1021/acsomega.3c04795
ACS Omega 2023, 8, 46490−46498

(4) To prepare 40 mL of acid solution, the acid solution was slowly added into the beaker with scale sample powder, then the beaker was put into a 90 °C water bath to react for 2 h.
(5) The reacted scale sample was filtered by the filter paper that has been weighed, and the filter paper and the scale sample powder were put into a dryer to dry, and the mass m_3 was weighed after cooling.
(6) The rate of dissolution of the acid on the scale sample was determined using the weight loss method and calculated as shown in eq 3.

$$V_2 = \frac{m_1 + m_2 - m_3}{m_2} \quad (3)$$

where V_2 is the scale sample dissolution rate, %; m_1 is the quality of filter paper, g; m_2 is the quality of the dirt sample, g; and m_3 is the weight of the filter paper and the remaining scale sample after the reaction, g.

2.6. Experiment on the Dissolution Ability of Acid on Rock Samples. The dissolution ability of the rock sample is the same as that of the scale sample except that the scale sample is replaced by about 5 g of core sample powder in the scale dissolution step, and the reaction temperature is reduced to 65 °C with 50 mL of dissolution acid.

2.7. Experimental Study on the Plugging Removal of Displacement Simulated Authigenic Acid Core. The displacement device is used to simulate the reservoir conditions under a certain temperature and pressure. During the experiment, the pumping sequence of field working fluid is simulated, mainly including the base fluid (simulated formation water), acidizing treatment fluid and base fluid.[25,26] The effect of acidizing plug removal is evaluated by observing the changes of core permeability before and after acidizing treatment. The schematic diagram of the device used in the displacement test is shown in Figure 2.

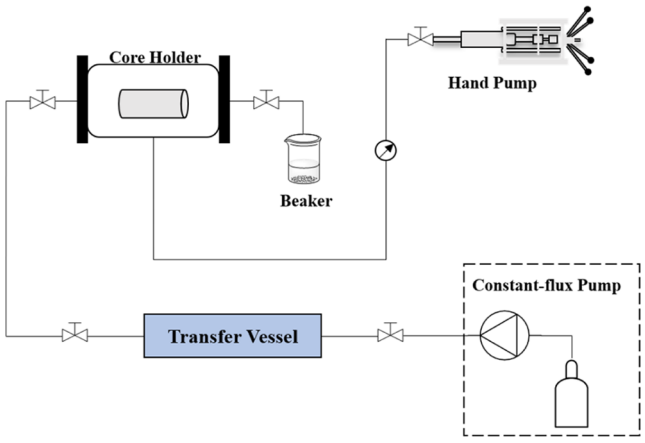

Figure 2. Schematic diagram of displacement simulation core blocking removal device.

3. RESULTS AND DISCUSSION

3.1. Evaluation of the Acid-Generating Ability of Autogenic Acid System. The acid-generating ability of autogenic acid is tested in the temperature range of 65−80 °C, and the results are shown in Figure 3. Figure 3a shows the curve of H^+ concentration with time from 1 to 30 min revealing the increase of the acid generation capacity of the autogenic acid system at different temperatures, and the acid generation rate and maximum H^+ concentration also increase with temperature. At 80 °C, the H^+ concentration in the acid solution reached 2.89 mol/L at 5 min, and then the H^+ concentration remained basically stable with the increase of time. At 30 min, the H^+ concentration only reached 3.02 mol/L. Figure 3b shows the curve of H^+ concentration with time from 30 to 180 min. When the experimental temperature reached 80 °C, it is not difficult to find that the H^+ concentration is 3.35 mol/L at 180 min, and these data will not change significantly after 30 min. When the time comes to 60 min, the H^+ concentration is basically stable. More importantly, the autogenic acid system can generate acid stably and continuously in 180 min, which means that acidizing and plugging removal can be carried out in the further well zone.

3.2. Experimental Evaluation of the Static Corrosion of Steel Sheet by Acid Solution. The atmospheric static corrosion rate of N80 steel was measured at 65 °C, and the results are shown in Table 1. The comparison experiment of the corrosion rate was carried out with acid solutions of different formulas. Among them, 10 wt % HCl + 3 wt % HF had the fastest corrosion rate to N80 steel, reaching 1.13 g/(m^2·h), followed by 10 wt % HCl, reaching 1.03 g/(m^2·h). The corrosion rate of authigenic acid is only 0.61 g/(m^2·h), and the corrosion rate decreases to 0.15 g/(m^2·h) after adding 2 wt % SA1-3B. It is not difficult to find that the corrosion rate of authigenic mud acid itself is lower than that of hydrochloric acid or 10 wt % HCl + 3 wt % HF mud acid system, and this data is further reduced after adding slow release agent.

As shown in Figure 4a, the corrosion of steel sheets by different acid systems can be easily distinguished from the pictures. Figure 4b shows the scanning electron microscopy (SEM) image of the steel sheet corroded by the acid-generating system. It can be found that the steel sheet surface has been corroded by acid at this time, and corrosion traces can be seen on the steel sheet surface. Figure 4c shows the SEM image for corrosion of steel sheet caused by autogenic acid plus 1 wt % SA1-3B. At this time, some corrosion traces appear on the surface of steel sheet, which has obvious change compared with the corrosion condition without inhibitor SA1-3B. Figure 4d shows the SEM image of steel sheet corrosion after autogenic acid plus 2 wt % SA1-3B. At this time, only slight corrosion can be found on the steel sheet surface, indicating that the corrosion inhibitor has a great effect on mitigating surface corrosion.

3.3. Experimental Evaluation of Scale Dissolution by Acid Solution System. SEM and energy-dispersive spectrometry (EDS) surface scanning analyses were carried out for the scale sample of a well in Bai-823 Block, and the results are shown in Figure 5. As shown in Figure 5a, it can be found that the scale sample is a black oil content substance, and SEM image shows that its composition is loose and amorphous, with disordered structure, and some areas are in continuous transition. It can be found from Figure 5b that the scale sample is mainly composed of C, O, S, Cl, Fe, Na, and Ca, and it is speculated that the scale sample is mainly composed of ferrous sulfide and some organic substances. Figure 5c shows the X-ray diffraction (XRD) image of the scale sample. After smoothing the spectrum, removing the copper target background, conducting database matching, and referring to the results of energy spectrum element analysis for phase retrieval, it was found that there may be FeS and NaCl present, and

https://doi.org/10.1021/acsomega.3c04795
ACS Omega 2023, 8, 46490−46498

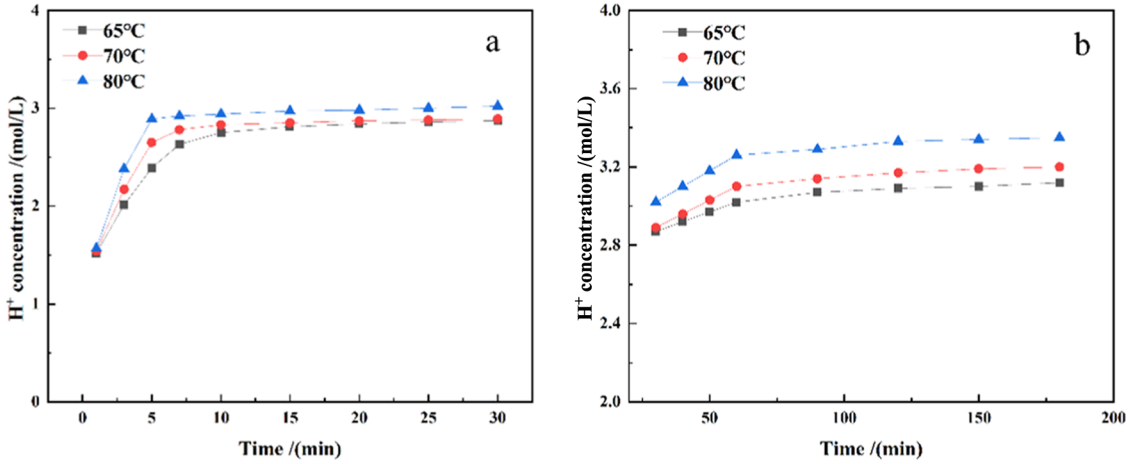

Figure 3. (a) 1−30 min; (b) time-varying curve of H^+ for 30−180 min.

Table 1. Test Results of 65 °C Atmospheric Static Corrosion Rate Measurement

acid type	area (mm^2)	mass before reaction (g)	mass after reaction (g)	corrosion rate ($g/(m^2 \cdot h)$)
10 wt % HCl + 3 wt % HF	1349.855	10.9223	10.9162	1.13
10 wt % HCl	1358.499	10.7537	10.7481	1.03
autogenic acid	1359.336	10.8482	10.8449	0.61
autogenic acid + 1 wt % SA1-3B	1372.233	11.0360	11.0340	0.36
autogenic acid + 2 wt % SA1-3B	1355.199	10.6626	10.6618	0.15

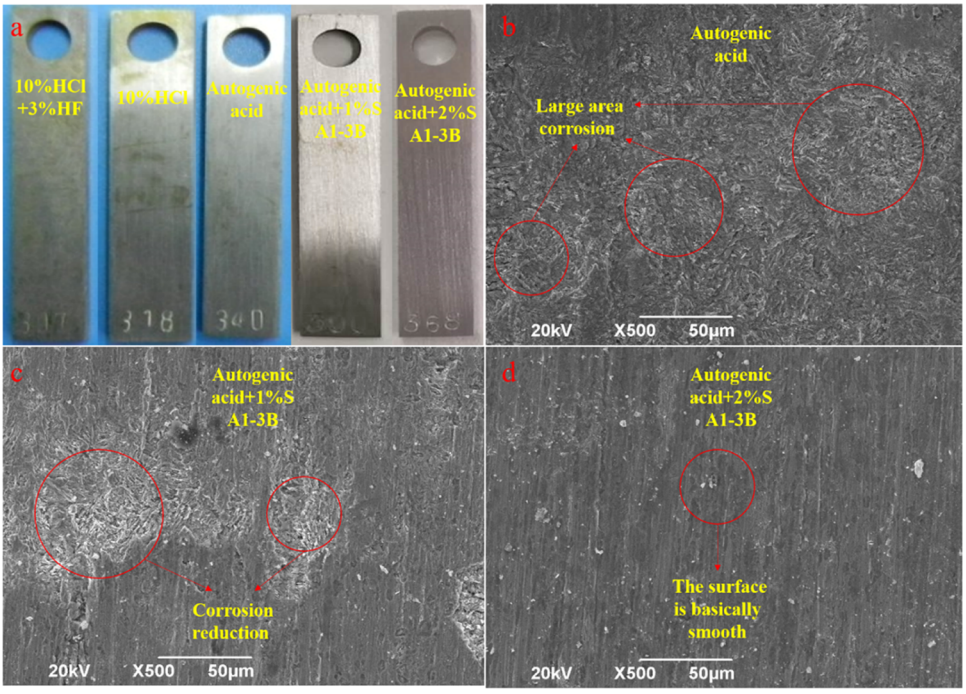

Figure 4. (a) Corrosion of steel sheets by different acid systems. SEM images: (b) autogenic acid, (c) autogenic acid + 1 wt % SA1-3B, (d) autogenous acid + 2 wt % SA1-3B steel sheet corrosion.

multiple parts of the spectrum have the best matching with the FeS standard spectrum, indicating that FeS is the main component in the blockage.

Table 2 shows the corrosion of scale samples by different acid systems. It is not difficult to see that when only hydrochloric acid is used to dissolve the scale sample, the corrosion rate of the scale sample gradually increases with the increase of hydrochloric acid concentration, but the growth rate of the corrosion rate is slow. This is because some substances in the scale sample, such as ferrous sulfide, have medium dissolution rates and dissolution rates in hydrochloric acid at 90 °C. When 10 wt % HCl + 3 wt % HF mud acid is used, the corrosion rate of the scale sample increases rapidly from 85.34% of 10 wt % HCl to 94.49%, indicating that the mud acid system can better solve the scale sample and has a better effect. When the authigenic acid system is used for scale sample dissolution, the dissolution rate is slightly lower than that of the 10 wt % HCl + 3 wt % HF mud acid system, which

https://doi.org/10.1021/acsomega.3c04795
ACS Omega 2023, 8, 46490−46498

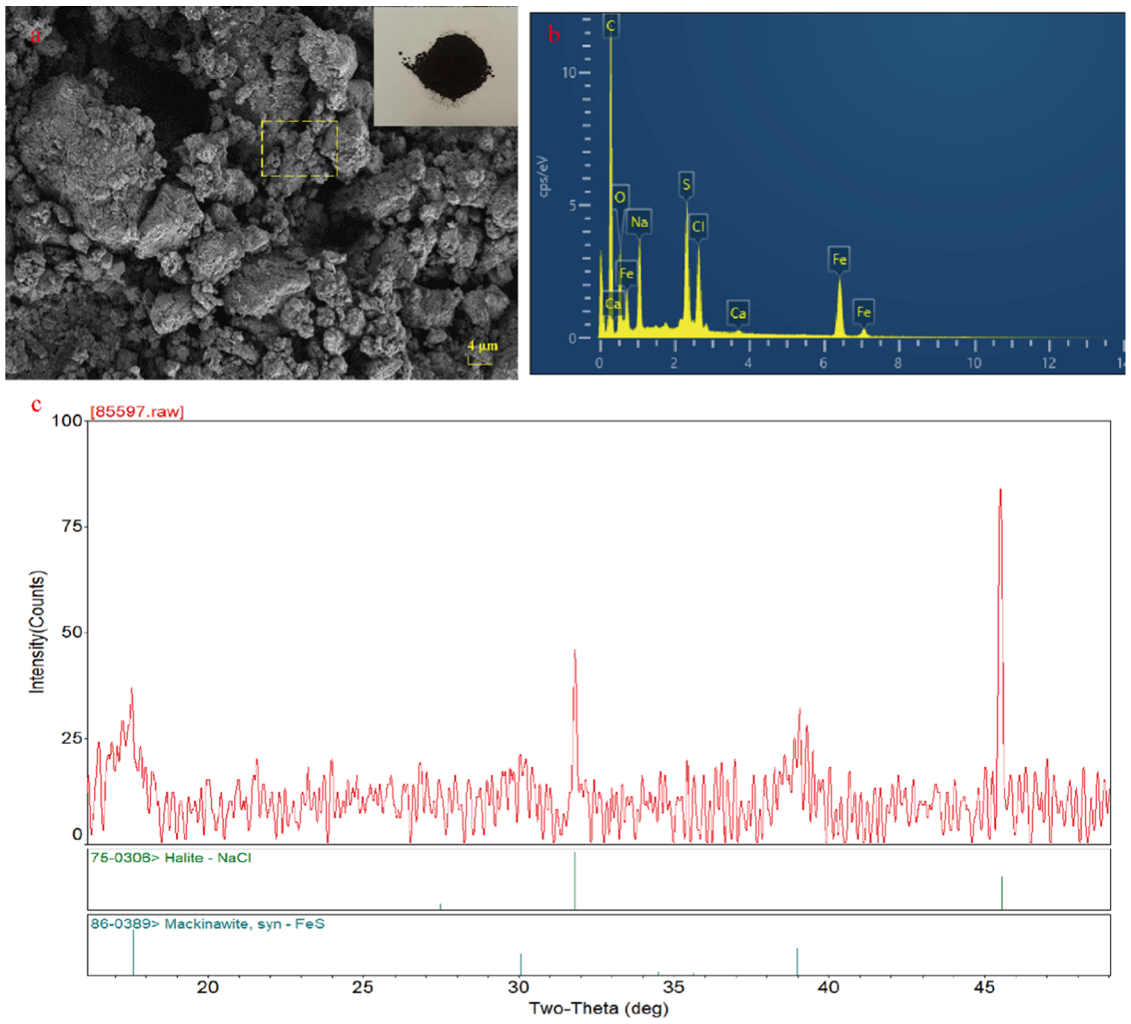

Figure 5. (a) SEM image; (b) EDS spectrum; (c) XRD pattern of scale sample.

Table 2. Corrosion of Scale Samples by Different Acid-Type Systems

acid type	filter paper weight (g)	weight before dissolution (g)	weight after dissolution (g)	reduce quality (g)	dissolution rate (%)
8 wt % HCl	1.0147	2.0412	1.3228	1.7331	84.91
10 wt % HCl	0.9730	2.0815	1.2781	1.7764	85.34
12 wt % HCl	0.9902	1.9952	1.2745	1.7109	85.75
10 wt % HCl + 3 wt % HF	0.9328	2.0325	1.0448	1.9205	94.49
autogenic acid	1.0320	2.0175	1.1568	1.8927	93.81

Table 3. Corrosion of Bai-823 Sandstone Samples by Acids with Different Acid Types

acid type	filter paper weight (g)	weight before dissolution (g)	weight after dissolution (g)	dissolution rate (%)
6 wt % HCl	0.9922	5.0383	5.3348	13.81
8 wt % HCl	0.9901	5.0090	5.3334	13.29
10 wt % HCl	0.9793	5.0093	5.3164	13.42
12 wt % HCl	0.9903	5.0063	5.3198	13.52
10 wt % HCl + 2 wt % HF	1.0288	5.0177	4.8163	24.52
10 wt % HCl + 3 wt % HF	1.0087	5.0386	4.6821	27.09
10 wt % HCl + 4 wt % HF	1.0055	5.0388	4.3722	33.18
autogenic acid	0.9831	5.0079	5.0205	19.38

is due to the slow and continuous release of H^+ in the authigenic acid system.

3.4. Experimental Evaluation of Acid Solution System on Core Dissolution. The core powder with a mass of about 5 g was weighed, and acid solutions with different formulas were used to evaluate the dissolution capacity. The results are shown in Table 3. When hydrochloric acid with different concentrations is used for treatment, the dissolution rate increases gradually with the increase of the hydrochloric acid concentration. The role of hydrochloric acid is mainly to

https://doi.org/10.1021/acsomega.3c04795
ACS Omega 2023, 8, 46490−46498

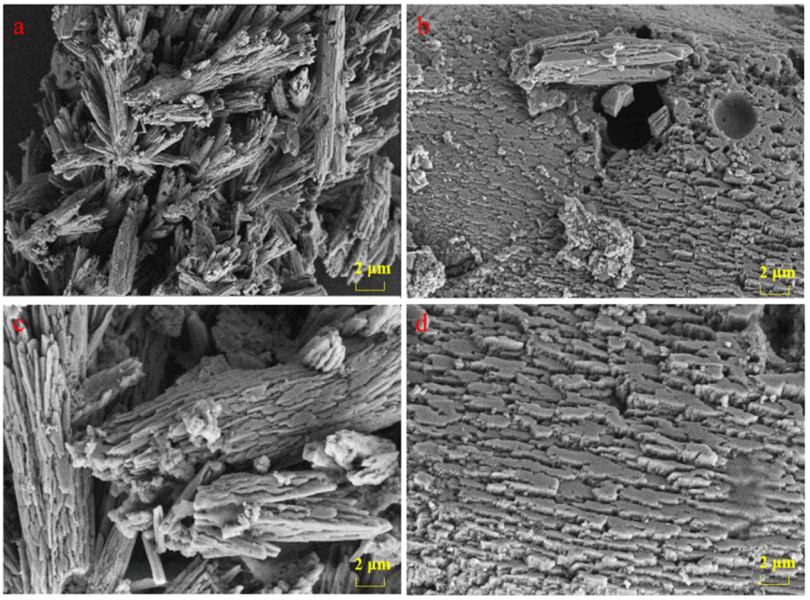

Figure 6. SEM images of (a) undissolved rock sample; (b) rock samples after dissolution in acid-generating system; (c) undissolved rock sample; (d) rock sample after dissolution of 10 wt % HCl + 3 wt % HF acid liquid system.

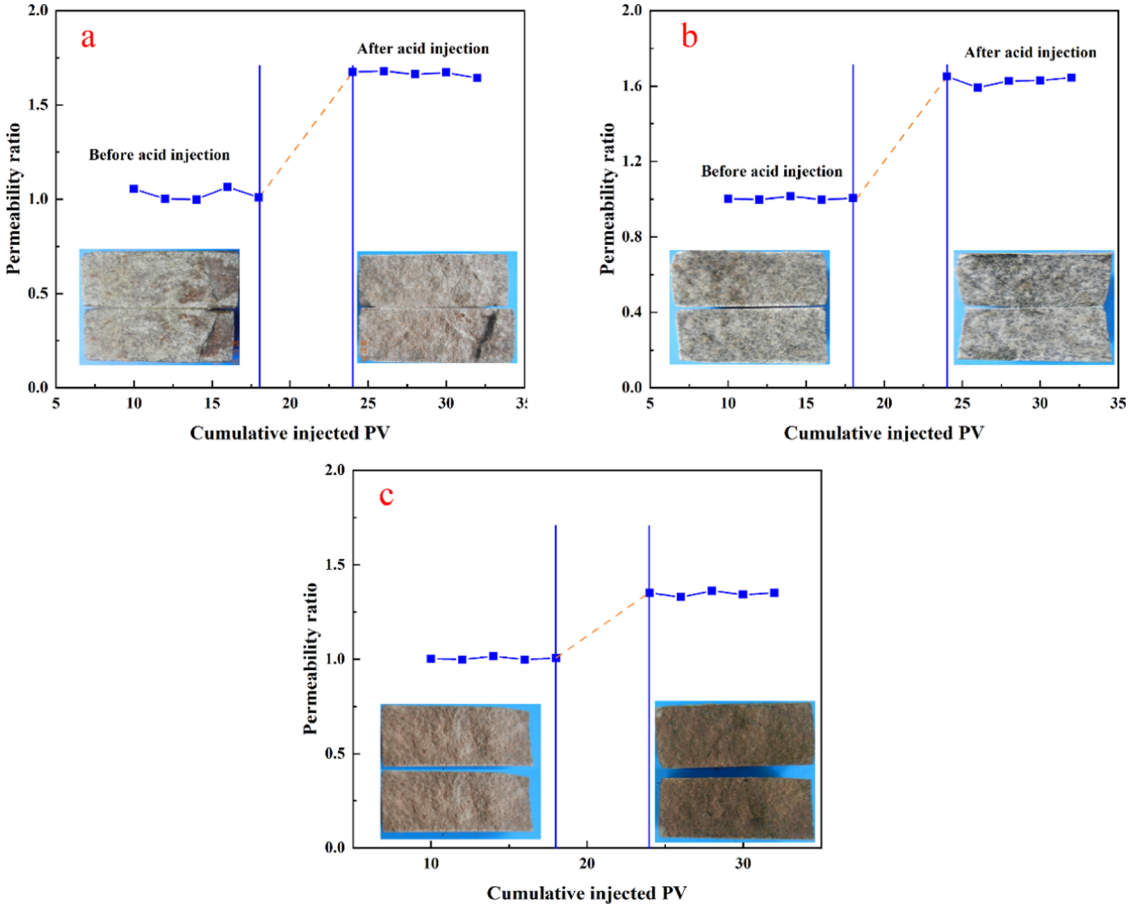

Figure 7. Permeability curve and cross section change diagram before and after mud acid treatment of (a) 10 wt % HCl + 3 wt % HF; (b) autogenic acid; and (c) 10 wt % HCl.

dissolve carbonate minerals, avoid the reaction between hydrofluoric acid and carbonate to produce calcium fluoride precipitation, and reduce the pH of the environment so as to effectively catalyze the dissolution of silicate rock minerals by hydrofluoric acid and prevent the generation of secondary sediment. When hydrofluoric acid is added to prepare mud acid, the dissolution rate of the acid solution system to core samples starts to increase rapidly. This is because mud acid can dissolve oil well plugging materials in addition to dissolving formation clay components, but mud acid has strong

https://doi.org/10.1021/acsomega.3c04795
ACS Omega 2023, 8, 46490−46498

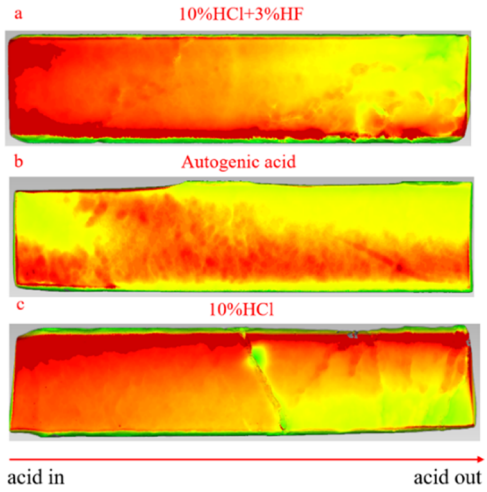

Figure 8. 3D laser scanning of rock core profiles corresponding to different acid solution systems after displacement reaction: (a) 10 wt % HCl + 3 wt % HF, (b) autogenic acid, (c) 10 wt % HCl.

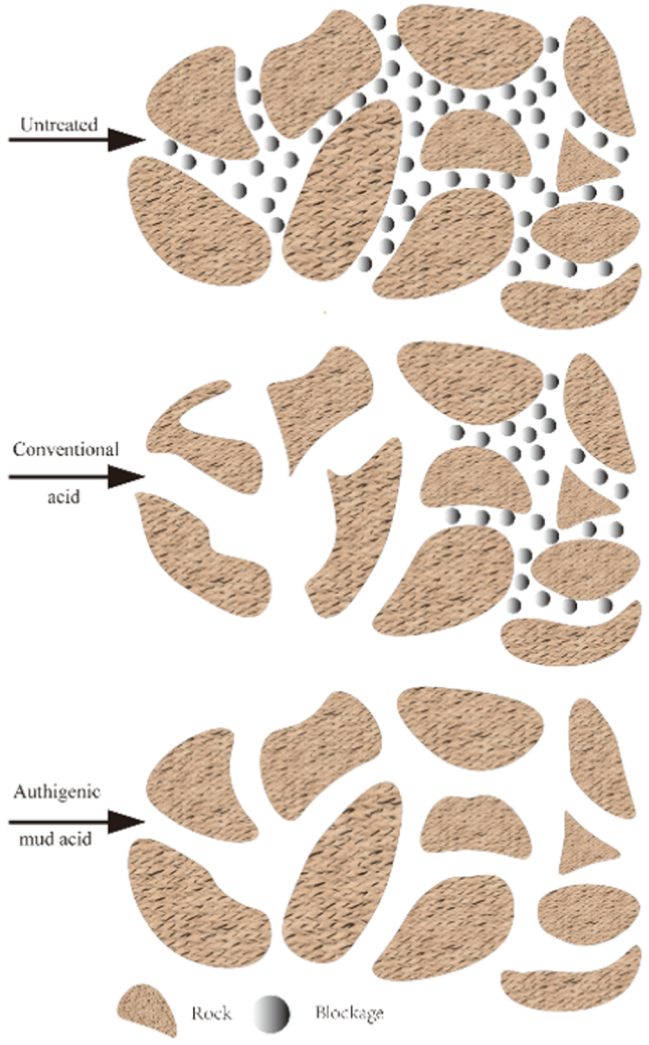

Figure 9. Core displacement plugging removal of different acid solution systems.

dissolution capacity and short action time and greatly reduces the strength of the rock skeleton. Compared with the general mud acid formula, the dissolution rate of authigenic mud acid decreases slightly because the acid generation of the authigenic acid system is a continuous process and the reaction is more mild than that of mud acid.

Figure 6a,c shows the SEM images of the rock sample before dissolution. At this time, it can be found that the surface of the rock sample is massive and fibrous and the surface is relatively uneven and undulating. Figure 6b shows the SEM image of the surface of the rock sample after the dissolution of the autogenic acid system. It is not difficult to find that only a small part of the fibrous and massive components remain on the surface of the rock sample, and the cave-like and strip-like traces of dissolution can be clearly observed. Figure 6d shows the SEM image of the rock sample surface after the dissolution of the 10 wt % HCl + 3 wt % HF mud acid solution system. At this time, no fibrous and blocky components can be seen on the rock sample surface. Instead, there are uniformly distributed traces of horizontal dissolution and cavernous dissolution, and the destructive capacity is obviously stronger than that of the authigenic mud acid system.

3.5. Evaluation of Core Displacement Plugging Removal Experiment. Figure 7 shows the result of a simulated acidizing plugging removal experiment of core displacement. Figure 7a shows the core permeability curve and profile diagram before and after the core is acidified with 10 wt % HCl + 3 wt % HF mud acid. First, the formation water simulated in the laboratory is used as the base fluid to measure the matrix permeability, and its value fluctuates around 1.00. After acid injection, the matrix permeability increases and fluctuates around 1.66, which indicates that the matrix permeability is displaced by acid solution, which can effectively improve the permeability of the rock core. Figure 7b shows the core permeability curve and profile diagram before and after the acidizing treatment of the core with the authigenic acid system. When the base fluid is used for treatment, its permeability also fluctuates around 1.00. Different from the mud acid with 10 wt % HCl + 3 wt % HF, its permeability fluctuates around 1.63 after the authigenic acid treatment and decreases slightly. Figure 7c shows the core permeability curve before and after acidification treatment with a 10 wt % HCl system and the profile diagram before and after displacement. When the core permeability fluctuates around 1.35 after treatment with 10 wt % HCl, it indicates that the plugging removal ability of the hydrochloric acid system is inferior to that of the autogenic acid system and general acid system.

At the same time, three-dimensional (3D) laser scanning was conducted on the core profile after the displacement reaction, and the differences in color depth in the image indicate differences in the height of the rock surface. As shown in Figure 8a, it is not difficult to find that there is a greater difference in the height of the core surface at the inlet end after using 10 wt % HCl + 3 wt % HF treatment, while the closer it is to the outlet end, the smaller the difference. As shown in Figure 8b, the core section after the autogenic acid treatment is smaller and more uniform. As shown in Figure 8c, the cross section of the treated core with 10 wt % HCl is similar to that of 10 wt % HCl + 3 wt % HF, with only a small difference at the inlet end. It is not difficult to draw a conclusion that the self-generated acid system has less damage to the rock core and can reach a more uniform distance from the injection end, which has greater advantages in removing blockages in remote well zones.

The schematic diagram of the core displacement plugging removal experiment for rock core displacement in Figure 9

https://doi.org/10.1021/acsomega.3c04795
ACS Omega 2023, 8, 46490−46498

shows that the autogenic acid system can achieve plug removal in the far wellbore area due to its slow and stable H^+ release rate, while the conventional acid system can only dissolve plugs within a small range, accompanied by significant core damage. This may cause some difficulty in hydraulic fracturing construction after acid plug removal.

4. CONCLUSIONS

(1) Aiming at problems such as low temperature and poor adaptability in the reservoirs, this article proposes an authigenic mud acid system of methyl formate, ammonium chloride, and ammonium fluoride. Compared with ordinary mud acid, it is more able to transform the far well zone at lower temperatures.

(2) The static corrosion test of N80 steel sheet and the corrosion ability was carried out in several different acid solution systems. It was found that authigenic mud acid system can dissolve scale samples faster, while causing less damage to steel sheet and rock core than other acid systems, indicating that authigenic mud acid is friendly to pipeline reservoirs and can effectively remove plugging.

(3) The displacement experiment is used to simulate the plugging removal process of acid solution. The results show that the plugging removal capacity of the hydrochloric acid system is inferior to that of the mud acid system, while authigenic mud acid and general mud acid do not have equal plugging removal capacity. However, since the displacement experiment is difficult to simulate remote well plugging removal, it is speculated that the remote well plugging removal capacity of authigenic mud acid should be superior to that of general mud acid.

AUTHOR INFORMATION

Corresponding Author

Chaozong Yan − *State Key Laboratory of Oil and Gas Reservoir Geology and Exploitation, Southwest Petroleum University, Chengdu 610500 Sichuan, China;* orcid.org/0009-0008-3750-9560; Email: ycz199605@163.com

Authors

Xiaolong Ni − *The Second Oil Production Plant, Xinjiang Oilfield Company, Karamay 834000 Xinjiang, China*

Runxin Cao − *The Second Oil Production Plant, Xinjiang Oilfield Company, Karamay 834000 Xinjiang, China*

Weifeng He − *The Second Oil Production Plant, Xinjiang Oilfield Company, Karamay 834000 Xinjiang, China*

Jinming Zhao − *State Key Laboratory of Oil and Gas Reservoir Geology and Exploitation, Southwest Petroleum University, Chengdu 610500 Sichuan, China*

Complete contact information is available at: https://pubs.acs.org/10.1021/acsomega.3c04795

Notes

The authors declare no competing financial interest.

ACKNOWLEDGMENTS

This work was supported by the National Natural Science Foundation of China (no. 51974264).

REFERENCES

(1) Zhang, Y.; Zhou, F.; Liu, Y. Influence Factors of Multifunctional Viscous Drag Reducers and Their Optimization for Unconventional Oil and Gas Reservoirs. *ACS Omega* **2021**, *6*, 32101−32108.

(2) Xiong, D.; Ma, X.; Yang, H.; Liu, Y.; Zhang, Q. Experimental and Numerical Simulation of Interlayer Propagation Path of Vertical Fractures in Shale. *Front. Energy Res.* **2021**, *9*, No. 797105.

(3) Liu, Z.; Pan, Z.; Li, S.; Zhang, L.; Wang, F.; Han, L.; Zhang, J.; Ma, Y.; Li, H.; Li, W. Study on the effect of cemented natural fractures on hydraulic fracture propagation in volcanic reservoirs. *Energy* **2022**, *241*, No. 122845.

(4) Zhao, Z. Y.; Lu, G. C.; Zhang, Y. H.; Lian, S. J.; Tian, N. Performance of EDAB-HCl Acid Blended System as Fracturing Fluids in Oil Fields. *Chin. J. Chem. Eng.* **2014**, *22*, 202−207.

(5) Ueda, K.; Matsui, R.; Ziauddin, M.; Teng, L. K.; Wang, W. K. Acid Selection for Volcanic Tuffaceous Sandstone with High Analcime Contents: A Laboratory Study in Kita-Akita Oil Field, Northern Japan. *SPE Prod. Oper.* **2021**, *36*, 1−21.

(6) Bisatto, R.; Picoli, V. M.; Petzhold, C. L. Evaluation of different polymeric scale inhibitors for oilfield application. *J. Pet. Sci. Eng.* **2022**, *213*, No. 110331.

(7) Chen, G. S.; Meng, Y. L.; Huan, J. L.; Wang, Y. C.; Zhang, L.; Xiao, L. H. Distribution and origin of anomalously high permeability zones in Weizhou formation, Weizhou 12-X oilfield, Weixinan Sag, China. *Earth Sci. Inf.* **2021**, *14*, 2003−2015.

(8) Abdel Ghany, N. A.; Shehata, M. F.; Saleh, R. M.; El Hosary, A. A. Novel corrosion inhibitors for acidizing oil wells. *Mater. Corros.* **2017**, *68*, 355−360.

(9) Kang, Y. L.; Xu, C. Y.; You, L. J.; Yu, H. F.; Zhang, B. J. Comprehensive evaluation of formation damage induced by working fluid loss in fractured tight gas reservoir. *J. Nat. Gas. Sci. Eng.* **2014**, *18*, 353−359.

(10) Shafiq, M. U.; Mahmud, H. K. B.; Zahoor, M. K.; Shahid, A.; Rezaee, R.; Arif, M. Investigation of change in different properties of sandstone and dolomite samples during matrix acidizing using chelating agents. *J. Pet. Explor. Prod. Technol.* **2019**, *9*, 2793−2809.

(11) Fayzi, P.; Mirvakili, A.; Rahimpour, M. R.; Farsi, M.; Jahanmiri, A. Experimental study of alcoholic retarded acid systems for high temperature gas wells acidizing process. *Chem. Eng. Res. Des.* **2015**, *93*, 576−583.

(12) Nazari Moghaddam, R.; Bokkers, A.; Aaldering, K.; Ferm, P.; Kooijman, C. In *New Retarded Acid System for High Temperature Applications: An Efficient Alternative to Emulsified and Viscosified Acid Systems*, SPE International Conference on Oilfield Chemistry, 2023.

(13) Abdrazakov, D.; Panga, M. K.; Daeffler, C.; Tulebayev, D. In *New Single-Phase Retarded Acid System Boosts Production after Acid Fracturing in Kazakhstan*, SPE International Conference and Exhibition on Formation Damage Control, 2018.

(14) Ravichandran, T.; Sidek, S.; Zakaria, A. N.; Ahmed Shata, K.; Sapiee, Z. N.; Abdul Rahman, H.; Foo Kwang Hui, N.; Wan Mohamad, W. A.; Yahaya, F.; Abdul Razak, A.; Maharon, D.; Jadid, M. In *Laboratory and Field Evaluation of Aqueous Retarded Acid System for Carbonate Gas Field, Offshore Borneo Island*, Abu Dhabi International Petroleum Exhibition & Conference, 2021.

(15) Lei, J. C.; Jia, J. P.; Liu, B. N.; Yan, W. Research and Performance Evaluation of an Autogenic Acidic Fracturing Fluid System for High-Temperature Carbonate Reservoirs. *Chem. Technol. Fuels Oils* **2021**, *57*, 854−864.

(16) Wang, Y.; Zhou, C. L.; Yi, X. Y.; Li, L.; Zhou, J.; Han, X.; Gao, Y. Research and Evaluation of a New Autogenic Acid System Suitable for Acid Fracturing of a High-Temperature Reservoir. *ACS Omega* **2020**, *5*, 20734−20738.

(17) Du, J.; Guo, G. X.; Liu, P. L.; Xiong, G.; Chen, P. F.; Liu, J. M.; Chen, X. Experimental Study on the Autogenic Acid Fluid System of a High-Temperature Carbonate Reservoir by Acid Fracturing. *ACS Omega* **2022**, *7*, 12066−12075.

(18) Wang, K. L.; Liu, G. Z.; Guo, Y. Y.; Yang, H.; Chen, Z. H.; Su, G. S.; Wang, Y. Q.; Wei, B.; Yu, X. R. Preparation and properties of degradable hydrogels as a temporary plugging agent used for acidizing

https://doi.org/10.1021/acsomega.3c04795
ACS Omega 2023, 8, 46490−46498

treatments to enhance oil recovery. *Colloids Surf., A* **2022**, *637*, No. 128218.
(19) Ji, Q.; Zhou, L.; Nasr-El-Din, H. Acidizing Sandstone Reservoirs With Aluminum-Based Retarded Mud Acid. *SPE J.* **2016**, *21*, 1050−1060.
(20) Mohamed, M.; Murtada, S. A.; Muhammad, S. K.; Syed, M. S. H. Sandstone acidizing using a new retarded acid system based on gemini surfactants. *J. Pet. Sci. Eng.* **2020**, *194*, No. 107459.
(21) Li, Y.; Zhou, F.; Li, B.; Cheng, T.; Zhang, M.; Wang, Q.; Yao, E.; Liang, T. Optimization of Fracturing Fluid and Retarded Acid for Stimulating Tight Naturally Fractured Bedrock Reservoirs. *ACS Omega* **2022**, *7*, 25122−25131.
(22) Zeegers-Huyskens, T.; Kryachko, E. S. Methyl formate and its mono and difluoro derivatives: conformational manifolds, basicity, and interaction with HF theoretical investigation. *J. Phys. Chem. A* **2011**, *115*, 12586−12601.
(23) Kim, J. Y.; Shin, I.; Byeon, J. W. Corrosion Inhibition of Mild Steel and 304 Stainless Steel in 1 M Hydrochloric Acid Solution by Tea Tree Extract and Its Main Constituents. *Materials* **2021**, *14*, No. 5016.
(24) Ricky, E. X.; Mpelwa, M.; Xu, X. G. The study of m-pentadecylphenol on the inhibition of mild steel corrosion in 1 M HCl solution. *J. Ind. Eng. Chem.* **2021**, *101*, 359−371.
(25) Fang, Y.; Yang, E.; Guo, S.; Cui, C.; Zhou, C. Study on micro remaining oil distribution of polymer flooding in Class-II B oil layer of Daqing Oilfield. *Energy* **2022**, *254*, No. 124479.
(26) Cui, K.; Xia, Y.; Tian, L.; Wang, S.; He, Y. Effect of supercritical CO;2;flooding on the produced water quality and performance of the scale inhibitors in a typical tight sandstone oilfield. *Pet. Sci. Technol.* **2022**, *40*, 1829−1840.

https://doi.org/10.1021/acsomega.3c04795
ACS Omega 2023, 8, 46490−46498